IEEE Access
Multidisciplinary | Rapid Review | Open Access Journal

Received February 14, 2018, accepted March 27, 2018, date of publication April 11, 2018, date of current version April 25, 2018.

Digital Object Identifier 10.1109/ACCESS.2018.2824839

Drone-Based Highway-VANET and DAS Service

HAFEZ SELIEM, REZA SHAHIDI, MOHAMED HOSSAM AHMED, AND MOHAMED S. SHEHATA

Department of Electrical and Computer Engineering, Memorial University of Newfoundland, St. John's, NL A1B 3X5, Canada

Corresponding author: Hafez Seliem (hms117@mun.ca)

This work was supported by the Natural Sciences and Engineering Research Council of Canada under Grant RGPIN 2014-03638.

ABSTRACT Wireless communications between vehicles are a focus of research in both the academic research community and automobile industry. Using unmanned aerial vehicles or drones in wireless communications and vehicular *ad hoc* networks (VANETs) have started to attract attention. This paper proposes a routing protocol that uses the infrastructure drones for boosting VANET communications to achieve a minimum vehicle-to-drone packet delivery delay. This paper also proposes a closed-form expression for the probability distribution of the vehicle-to-drone packet delivery delay on a two-way highway. In addition, based on that closed-form expression, we can calculate the minimum drone density (maximum separation distance between two adjacent drones) that stochastically limits the worst case of the vehicle-to-drone packet delivery delay. Moreover, this paper proposes a drones-active service that is added to the location service in a VANET. This service dynamically and periodically obtains the required number of active drones based on the current highway connectivity state by obtaining the maximum distance between each two adjacent drones while satisfying a probabilistic constraint for vehicle-to-drone packet delivery delay. Our analysis focuses on two-way highway VANET networks with low vehicular density. The simulation results show the accuracy of our analysis and reflect the relation between the drone density, vehicular density and speed, other VANET parameters, and the vehicle-to-drone packet delivery delay.

INDEX TERMS Vehicular network, VANET, unmanned aerial vehicles, drones, probability density function, end-to-end delay, two-way, analytical.

I. INTRODUCTION

Wireless communications between vehicles is a focus of research in both the academic research community and automobile industry. Many vehicle manufacturers have equipped their new vehicles with global positioning systems (GPSs) [1] and wireless communication devices. Vehicular ad-hoc network (VANET) technology enables ad-hoc communication between vehicles, or vehicles and fixed infrastructure-roadside units (RSUs) through wireless communication devices installed on the vehicles. VANETs are currently a widely-discussed and researched area in wireless communications. Moreover, the United States Federal Communications Commission (FCC) has allocated 75 MHz of the radio spectrum at 5.9 GHz to be used by Dedicated Short Range Communications (DSRC) [2]. DSRC is a short-to-medium-range communications service that was developed to provide vehicle-to-roadside and vehicle-to-vehicle (V2V) communications. Moreover, DSRC are aimed at providing communications with a high data rate and low end-to-end delay.

VANETs have many applications; the most important of them are active safety applications that can be used to assist drivers to avoid collisions and to coordinate between them at crowded intersections and highway entries [3]. Moreover, VANETs can intelligently detect and convey road status information, such as real-time traffic congestion, average speed, surface condition, or high-speed tolling, to vehicles in the vicinity of specific sites. Moreover, VANETs also provide comfort applications to users, for example: mobile e-commerce, weather information, Internet access and many other multimedia applications.

Some VANET applications place more emphasis on hard delay constraints than high data rates. For example, for accident avoidance applications where certain events such as air bag ignition or brake events occur, the message must be delivered in a certain amount of time to avoid more accidents. Therefore, it is important to calculate the probability distribution of the VANET delay or determine its statistics (e.g., CDF, moments, and characteristic function).

The high mobility of vehicles is the main and most critical factor in VANET systems. The mobility of vehicles is affected by driver behavior, and constraints on mobility such as roads, road restrictions and junctions, traffic lights and high speeds.

We need to consider these characteristics for design decisions in such networks. There are two typical communication scenarios in which VANETs operate. The first scenario is a highway scenario where the environment is straightforward without obstacles. The second scenario is an urban scenario where vehicles are often separated by buildings, trees, and other obstacles.

Many papers have proposed connectivity analysis (propagation speed and time) and delay probability distribution for vehicle-to-infrastructure (V2I) communications in VANETs based on fixed infrastructure-RSUs. For instance, Abdrabou and Zhuang [4] proposed a probabilistic model for vehicle-to-RSU packet delivery delay. Their model is based on effective bandwidth theory and the effective capacity concept in order to obtain the maximum distance between infrastructure-RSUs that stochastically limits vehicle-to-RSU packet delivery delay to a certain upper bound.

In addition, a mathematical framework for the vehicle-to-RSU packet delivery delay distribution based on the distance between fixed RSUs that is uniformly distributed over the road was proposed in [5]. However, they did not consider the RSU wireless communication coverage in their model.

Moreover, Jeong *et al.* [6] proposed a trajectory-based data forwarding scheme, tailored for data forwarding for roadside reports in sparse VANETs. They derived the expected end-to-end delivery delay from a vehicle to Internet access points. Additionally, He *et al.* [7] proposed an analytical framework for the expected path delay in bidirectional vehicular traffic. Using this analytical model, a shortest-path algorithm was applied to select the path with the lowest expected delay.

On the other hand, an optimal infrastructure-RSU-placement model for hybrid VANET sensor networks was proposed in [8]. It applies the center particle swarm optimization approach after it formulates the problem as an integer linear-programming optimization problem. In addition, [9] presents an analysis for the total delay of broadcasting alert messages in VANETs along a highway such that alert messages can be transmitted to the nearest RSU within a given delay bound. They derived a closed-form expression for the expected value of the total delay of broadcasting alert messages based on the distance between RSUs.

Unmanned aerial vehicles (UAVs) or drones are semi-autonomous or fully-autonomous unmanned aircrafts that have storage space and some on-board intelligence. Therefore, drones can be equipped with communication devices which makes them a possible option to improve connectivity and efficiency for many communication systems. Integration of wireless communication systems and UAVs has started to attract attention. For instance, Bor-Yaliniz and Yanikomeroglu [10] proposed drone-base-stations (drone-BSs) that can be used in cellular wireless networks. Consequently, drone-BSs provide a dynamic deployment ability that offers service where the demand exists. In addition, the drone-cell size depends on many parameters (e.g., UAV altitude, spectrum frequency, environment, and the transmitted power).

Many papers have proposed their solutions for integrating drones in wireless communication systems. On the other hand, only a few papers have proposed using drones in VANETs. For instance, Wang *et al.* [11] proposed VDNet as a routing protocol for vehicle-to-vehicle (V2V) communications based on drones to decrease the average end-to-end packet delivery delay. In VDNet, some vehicles are equipped with an on-board drone, which can relay messages in a multi-hop route, deliver data messages directly to the destination, and collect location information while flying above the traffic.

Moreover, [12] proposed connectivity-based traffic density aware routing using UAVs (CURVE) as a routing protocol for VANETs in urban scenario using drones through cooperative and collaborative communication. The drones exchange information with the vehicles to select the most appropriate next intersection to deliver the data packets successfully to their destinations.

In addition, Oubbati *et al.* [13] proposed an intersection UAV-assisted VANET routing protocol (UVAR) that uses drones. UVAR is based on the drones collecting information about the state of the vehicles' connectivity, and exchanging this information with vehicles through "Hello" messages. Moreover, when a VANET has a gap (connectivity between vehicles on the ground is not possible as the distance between two vehicles is greater than the vehicle wireless communication range), UVAR uses the drones as a relay.

This paper proposes a routing protocol for V2I communications where we replace the infrastructure RSUs with infrastructure drones. While, the vehicles transmit their real-time information and Internet requests to the infrastructure drones, the drones represent gateways to the Internet and the infrastructure of other systems such as the intelligent transport system (ITS). However, it is difficult, in terms of infrastructure cost (number of drones), to get VANETs with full connectivity by covering all gaps in the highway. On the contrary, using a small number of drones causes long vehicle-to-drone delays due to having to carry packets for a longer distance, especially in VANETs with low vehicular density. This is because the vehicles use the carry-and-forward strategy through these gaps until reaching the next drone. This paper proposes a closed-form expression to characterize the vehicle-to-drone delay probability distribution in bidirectional highway VANETs with low vehicular density where the sensed data packet is destined to the infrastructure drones.

The closed-form expression of vehicle-to-drone packet delivery delay probability distribution offers a design tool that can determine the maximum separation distance between two adjacent drones while satisfying a probabilistic requirement of vehicle-to-drone packet delivery delay. Consequently, we can calculate the minimum number of drones required to cover a two-way highway road. Moreover, it can be used for the optimization of drone placement. In this paper, we use this closed-form expression to change the drones' locations based on the highway connectivity state. The proposed

closed-form expression takes into account the likelihood of a carrier vehicle exiting the road at any road junction, the spatial distribution of road junctions, the vehicular density over the highway, and the drone communication range.

The main contributions of this paper are as follows: 1) it analyzes the drone wireless communication coverage in VANETs based on the drone altitude and the other environment communication parameters, 2) it proposes a closed-form expression of the vehicle-to-drone packet delivery delay probability distribution for the proposed protocol and reflects the relation between the vehicle-to-drone packet delivery delay and the drone density, 3) it proposes an algorithm to determine the minimum required number of active drones based on the current state of the vehicles connectivity while satisfying a probabilistic requirement for vehicle-to-drone packet delivery delay, and 4) it compares results from the proposed closed-form with simulation results to show the accuracy of our analysis.

The rest of this paper is organized as follows. Section II introduces the system model. Section III discusses the drone wireless communication coverage in VANETs. Section IV presents the problem formulation and the closed-form expression for characterizing the vehicle-to-drone packet delivery delay probability distribution. In addition, Section V proposes a drones-active service to determine the minimum required number of active drones based on the current highway state. Next, Section VI compares simulation results against analytical results. Finally, the conclusions and future work are presented in Section VII.

II. SYSTEM MODEL

In our analysis, we consider a two-way highway with vehicles moving in one of two opposite directions as shown in Fig. 1. In addition, each direction is a straight line with a fixed length of a meters and has two drones, one at each end. Moreover, the vehicles are moving in the forward and opposite directions with a constant speed of v_f and v_b, respectively. The constant speed assumption over the observation period helps to investigate the worst case scenario in V2Is where vehicles moving in one direction have the same speed between two adjacent drones (we do not consider vehicles overtaking other vehicles). In addition, y is the distance that the vehicle travels while carrying the packet before forwarding to the next drone as shown in Fig. 1.

Moreover, we assume the road junctions are distributed randomly on the highway as depicted in Fig. 1. Some vehicles may join and others may leave at any road junction along the highway. In addition, we assume that the number of road junctions within the highway follows a Poisson distribution with a parameter λ_c and a vehicle can leave the highway at any road junction with a probability P_c as assumed in [5].

Additionally, we assume the inter-vehicular distances between the vehicles are exponentially distributed [4], [14], and the number of vehicles in each direction is Poisson-distributed with vehicular densities λ_f and λ_b for the forward and backward directions, respectively. In a more realistic VANET scenario, the vehicular density and the vehicle exit probability at the road junctions change with time. For instance, at the junction of a big company or a city, the probability of vehicle exit in the morning (people go to their work) or the end of the day (people return back from their work) is higher than other times (at the night period). Therefore, the drones can change their placement and the inter-drone distance while satisfying the probabilistic constraint of the vehicle-to-drone packet delivery delay based on the current highway state.

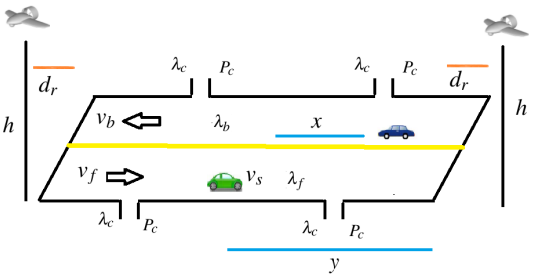

FIGURE 1. System model for bidirectional highway.

TABLE 1. List of notation.

a	Gap between two consecutive drones
d_r	Vehicle wireless communication range
X	R.V. for inter-vehicle distance
Y	R.V. for distance between a vehicle and the drone
θ	End-to-end propagation delay
P_{LoS}	The carrier frequency
c	The speed of light
P_{NLoS}	The probability of non-LoS connection
h	The drone's altitude
r	The distance between a vehicle and a drone
$F_{T_c}(t)$	CDF of T_c
$f_{T_c}(t)$	PDF of T_c
λ	Traffic flow rate (vehicles/unit time)
λ_f	Exponential mean distance in the forward direction
λ_b	Exponential mean distance in the backward direction
λ_c	The expected number of junctions
P_c	The probability that vehicle exits at any junction
v_f	Speed for the forward direction
v_b	Speed for the backward direction
$u(\cdot)$	Heaviside unit step function

In addition, we assume that the source of packets is any moving vehicle and the destination is an infrastructure drone which has access to the Internet and other infrastructure systems. In addition, a vehicle acting as the packet source sends one replica of the packets in the opposite direction of the highway. Therefore, packets are carried either by their source vehicles or a carrier vehicle moving in the opposite direction of the highway. In the case of high vehicular density, a connected multihop vehicle-to-drone path can be found with a high probability; however, this case is out of the scope of the proposed work. Our analysis focuses on the worst case where the original packet is stored by its source vehicle until it is within the communication range of the next drone.

Moreover, we assume that the VANET includes a location service such as a hierarchical location service (HLS) [15] or grid location service (GLS) [16]. Moreover, the transmission range between vehicles is assumed to be smaller

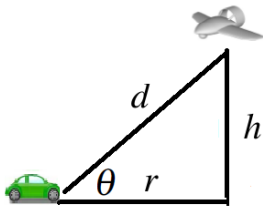

FIGURE 2. Air-to-ground path-loss model.

than the distance between two adjacent drones a. In addition, we assume that the medium access control (MAC) layer protocol is the distributed coordination function (DCF) of the IEEE 802.11 standard. Finally, it is assumed that the packet traffic model follows the constant bit rate (CBR) pattern between a source vehicle and an infrastructure drone.

III. DRONE WIRELESS COMMUNICATION COVERAGE

There is a growing number of papers related to the wireless communication range of drone base-stations (BSs) in cellular networks. For instance, Al-Hourani *et al.* [17] proposed an air-to-ground path-loss model for low altitude platforms (LAPs), like drone-BSs at heights of less than 3 km. In their model, there are two main propagation categories, corresponding to the receivers with line-of-sight (LoS) connections and the ones without LoS (NLoS) connections which the receivers still receive the signal from LAPs due to strong diffractions and reflections.

Moreover, [18] proposed a channel path-loss model for drone-BSs in urban areas with respect to intersections and roof-top heights of buildings. It adopts an ITU channel model by optimizing parameters of the selected ITU model such that it can be used for altitudes both strictly lower and higher than building roof-tops.

In addition, the optimal altitude of a single drone-BS to obtain a required wireless communication coverage while minimizing the transmit power is found in [19]. Moreover, a closed-form expression for the probability of LoS connection between a LAP and a receiver is proposed in [20] and formulated as follows

$$P_{LoS} = \frac{1}{1 + e^{-b(\frac{180}{\pi}\theta - a)}}, \tag{1}$$

where a and b are constant values depending on the environment (rural, urban, etc), and θ is the elevation angle. This elevation angle is equal to $\arctan(\frac{h}{r})$, where h and r are the drone's altitude and its horizontal distance from the vehicle, respectively as shown in Fig. 2, Eq. (1) shows that the probability of having a LoS connection is increased as the elevation angle increases. Consequently, the probability of LoS will increase, if the drone altitude increases for a fixed r.

On the other hand, based on [20], the mean path-loss channel model for drone-to-vehicle communications will be

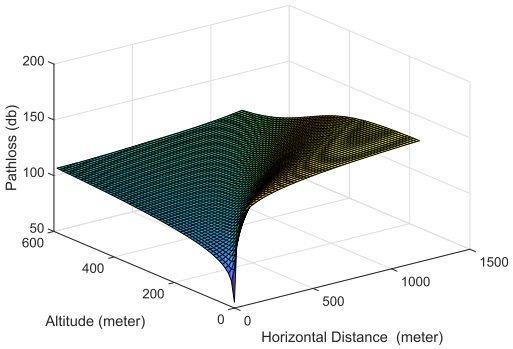

FIGURE 3. 3D plot between the drone's altitude, the drone's horizontal distance, and path-loss.

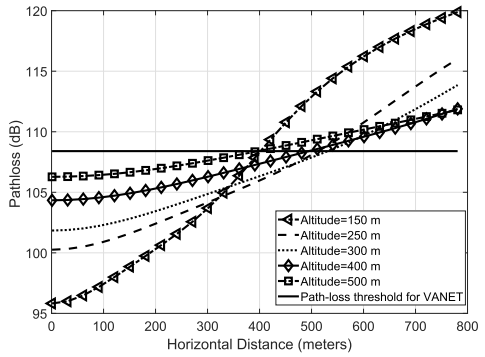

FIGURE 4. Path-loss for different drone altitudes.

as follows

$$PL(dB) = 20\ \log_{10}\left(\frac{4\pi f_c d}{c}\right) + P_{LoS}\ \eta_{LoS} + P_{NLoS}\ \eta_{NLoS}, \tag{2}$$

where c is the speed of light, f_c is the carrier frequency, and the probability of non-LoS connection $P_{NLoS} = 1 - P_{LoS}$. Moreover, d is the distance between the drone and the vehicle that is equal to $\sqrt{h^2 + r^2}$ as shown in Fig. 2. In addition, η_{LoS} and η_{NLoS} depend on the environment and they are the average additional loss to the free space propagation for LoS and NLoS connections, respectively.

Therefore, in a VANET, the wireless communication coverage for the drones depends on the drone altitudes, the path-loss threshold in the VANET, and the carrier frequency f_c.

Based on Eq. (1) and Eq. (2), Fig. 3 shows a 3D plot between the drone's altitude, the drone's horizontal distance from the vehicle, and the mean path-loss propagation channel for drone-to-vehicle communication where $a = 9.6$, $b = 0.28$ as in [19], and $f_c = 5.9$ GHz. It is noticed that an increase in drone altitude does not always lead to an increase in the mean-path loss. There is a decrease in the mean path-loss when the drone altitude is between 200 meters and 400 meters for the same horizontal distance.

On the other hand, based on Eqs. (1) and (2), Fig. 4 shows the mean path-loss propagation channel for drone-to-vehicle communication against the horizontal distance between the vehicle and the drone altitudes where $a = 9.6$, $b = 0.28$ as in [19], and $f_c = 5.9$ GHz. Moreover, we use diffrent drone

altitudes: 150, 250, 300, 400, and 500 meters. In additon, based on experimental results, Fernández *et al.* [21] found the mean path-loss threshold for VANETs at $f_c = 5.9$ GHz and 750 MHz. The path-loss threshold for $f_c = 5.9$ GHz in [21] is 108 dB.

Therefore, the drone wireless communication coverage at any altitude in Fig. 4 is found by obtaining the intersection point between the mean path-loss threshold line and the drone altitude line. It is noticed that the wireless communication range for a drone altitude of 150 and 500 meters is close to 400 meters. On the other hand, the wireless communication range for a drone altitude of 300 meters is close to 540 meters. In addition, the main factor affecting the optimal altitude is the mean path-loss threshold. For instance, if we were to change the mean path-loss threshold to 110 dB, the optimal altitude would be at 400 meters and the range would be close to 640 meters.

The reason behind this behavior in both figures is that at low drone altitudes the probability of NLoS becomes greater than that of LoS, due to reflections by buildings and other obstacles, and the additional loss of a NLoS connection is higher than a LoS connection. However, when the drone's altitude increases, the LoS probability increases as well and in turn mean path-loss decreases. On the contrary, the mean path-loss is also dependent on the distance between the vehicle and the drone. Consequently, after a specific height, the distance between the vehicle and the drone factor dominates the mean path-loss. Therefore, after this specific height, when the drone altitude increases, the mean path-loss increases.

IV. PROBLEM FORMULATION AND THE ANALYSIS

In this section, we follow the same methodology proposed in [5]. However, in this paper, the drone wireless communication range d_r is considered in the model, while, Abdrabou *et al.* [5] did not consider the wireless communication range for the RSU. In this paper, we aim to obtain a closed-form expression for the vehicle-to-drone packet delivery delay cumulative distribution function (CDF) $F_T(t)$ in terms of a (the distance between each pair of adjacent drones), d_r (drone wireless communication range that depends on drone altitude and mean path-loss threshold), road-junction density and probability of vehicles exit at those junctions, and vehicular density on the two-way highway road as shown in Fig. 1. Using this closed form, we can obtain the minimum number of drones (maximum a) that satisfies a certain vehicle-to-drone delay constraint $T_{\max}$ with a violation probability of at most ϵ as follows

$$\begin{aligned} &\text{maximize } a \\ &\text{subject to } 1 - F_T(T_{\max}, a) \leq \epsilon. \end{aligned} \tag{3}$$

As we mentioned in the system model, we consider in the model that the source vehicle sends the packet in the forward and opposite directions (two replicas of the same packet) and consider the packet that reaches the infrastructure earlier. Consequently, the vehicle-to-drone packet delivery delay will be less than if we were to just transmit the packet in one direction. Therefore, the probability that the vehicle-to-drone packet delivery delay T is less than t can be formulated as follows

$$Pr(T \leq t) = Pr(T \leq t, I = 1) + Pr(T \leq t, I = 0), \tag{4}$$

where T is a random variable representing the vehicle-to-drone packet delivery delay and I is a random variable representing the number of extra replicas of the packet. In addition, the first term $Pr(T \leq t, I = 1)$ represents the case when the source vehicle sends the packet in the forward and opposite directions. On the other hand, the second term $Pr(T \leq t, I = 0)$ represents the case when the source carrier vehicle sends the packet only in the forward direction.

First, we need to get a closed-form expression for the term $Pr(T \leq t|I = 1)$ (the conditional CDF of the vehicle-to-drone packet delivery delay given $I = 1$). It can be formulated as follows

$$Pr(T \leq t, I = 1) = Pr(T \leq t|I = 1)Pr(I = 1). \tag{5}$$

Moreover, from Fig. 1, we can limit Y (the distance between the source vehicle and the drone in the forward direction) to be between 0 and $(a - 2d_r)$. On the other hand, X (the distance between the source vehicle and the first vehicle in the opposite direction) will be between 0 and ∞. Therefore, Eq. (5) can be expressed as follows

$$\begin{aligned} Pr(T \leq t, I = 1) = &\int_0^{\infty} \int_0^{a-2d_r} Pr(T \leq t|I=1, X=x, Y=y) \\ &Pr(I = 1|X = x, Y = y) f(x, y)\, dy\, dx, \end{aligned} \tag{6}$$

where d_r is the drone communication range. Moreover, the first term $Pr(T \leq t|I = 1, X = x, Y = y)$ represents the probability the delay T is less than t conditioned on one replica of the packet in the opposite direction besides the original copy in the forward direction. This term can be formulated as follows

$$\begin{aligned} &Pr(T \leq t|I = 1, D = \delta, X = x) \\ &\quad = u\left(t - \min\left(\frac{a - \delta - d_r + x}{v_b}, \frac{y - d_r}{v_f}\right)\right), \end{aligned} \tag{7}$$

where $u(\cdot)$ is the Heaviside unit step function. In addition, we can remove min(·) in Eq. (7) as follows

$$\begin{aligned} &Pr(T \leq t|I = 1, D = y, X = x) \\ &= \begin{cases} u\left(t - \dfrac{y - d_r}{v_f}\right), \\ \text{if } 0 \leq y \leq \min\left(\dfrac{(a - d_r + x)v_f + d_r v_b}{v_b + v_f}, a - 2d_r\right), \\ u\left(t - \dfrac{a - y - d_r + x}{v_b}\right), \\ \text{if } \min\left(\dfrac{(a-d_r+x)v_f + d_r v_b}{v_b+v_f}, a-2d_r\right) \leq y \leq a - 2d_r. \end{cases} \end{aligned} \tag{8}$$

On the other hand, the term $f(x, y)$ is the joint probability density function (PDF) of X and Y. In addition, Y is uniformly distributed since the vehicle location is uniformly distributed over the range $[0, a-2d_r]$. On the contrary, as we mentioned in the system model, the inter-vehicle distance, X, is exponentially distributed since the vehicles form a Poisson process. Consequently, we can obtain the expression for $f(x, y)$ as follows

$$f(x,y) = \frac{\lambda_f + \lambda_b}{a-2d_r} e^{-(\lambda_f+\lambda_b)x}, \quad x > 0. \tag{9}$$

Moreover, the term $Pr(I = 1|X = x, Y = y)$ represents the probability that the packet carrier vehicle will not leave the highway at any road junction. As we mentioned in the system model, we assume that a vehicle can leave the highway at any road junction with a probability P_c and the number of road junctions within the highway follows a Poisson distribution with a parameter λ_c. Therefore, within a distance of y, the vehicle will leave with probability $P_l(y)$, where $P_l(y) = 1 - e^{-\lambda_c P_c y}$ as proposed in [5]. As a result, the probability that the packet carrier vehicle will not leave the highway at any road junction can be expressed as follows

$$Pr(I = 1|X = x, Y = y) = e^{-\lambda_c P_c (a-\delta-d_r+x)}. \tag{10}$$

Finally, by substituting Eq. (8) and Eq. (10) into Eq. (6), we can formulate the first term on the right side on Eq. (4) as follows

$$\begin{aligned} Pr(T \le t, I = 1) = &\int_0^{\infty} f(x,y) \int_0^{m} \\ &\times u\left(t - \frac{y-d_r}{v_f}\right) e^{-\lambda_c P_c (a-y-d_r+x)} dy\, dx \\ &+ \int_0^{\infty} f(x,y) \int_m^{a-2d_r} u\left(t - \frac{a-y-d_r+x}{v_b}\right) \\ &\times e^{-\lambda_c P_c (a-y-d_r+x)} dy\, dx, \end{aligned} \tag{11}$$

where $m = \min\left(\frac{(a-d_r-y+x)v_f + d_r v_b}{v_b+v_f},\ a-2d_r\right)$.

Moreover, we can remove the min(·) term in the integration. In this case, Eq.(11) can be formulated as follows

$$\begin{aligned} Pr(T \le t, I = 1) = &\int_0^{b_1} \int_0^{b_2} k_1\, dy\, dx \\ &+ \int_{b_1}^{\infty} \int_0^{a-2d_r} k_1\, dy\, dx + \int_0^{b_1} f(x,y) \\ &\times \int_{b_2}^{a-2d_r} u\left(t - \frac{a-y-d_r+x}{v_b}\right) \\ &\times e^{-\lambda_c P_c (a-y-d_r+x)} dy\, dx, \end{aligned} \tag{12}$$

where

$$k_1 = f(x,y) u\left(t - \frac{y-d_r}{v_f}\right) e^{-\lambda_c P_c (a-y-d_r+x)},$$

and

$$b_1 = \frac{a v_b - d_r(v_f+3v_b)}{v_f},\ b_2 = \frac{(a-d_r-y+x)v_f + d_r v_b}{v_b+v_f}.$$

On the contrary, we need to obtain a closed-form expression for the second term on the right side of Eq. (4) in the case of $I = 0$, where there is no replica for the packet in the opposite direction. This term can be formulated as follows,

$$\begin{aligned} Pr(T \le t, I = 0) = &\int_0^{\infty} \int_0^{a-2d_r} Pr(T \le t|I=0, X=x, Y=y) \\ &Pr(I = 0|X = x, Y = y) f(x,y)\, dy\, dx, \end{aligned} \tag{13}$$

where the term $Pr(T \le t|I = 0, D = y, X = x)$ will be

$$Pr(T \le t|I = 0, D = y, X = x) = u\left(t - \frac{y-d_r}{v_f}\right). \tag{14}$$

$$\begin{aligned} Pr(T \le t) = &\int_0^{b_1} m_1 \int_0^{b_2} u\left(t - \frac{y-d_r}{v_f}\right) m_2\, dy\, dx + \int_{b_1}^{\infty} m_1 \int_0^{a-2d_r} u\left(t - \frac{y-d_r}{v_f}\right) m_2\, dy\, dx + \int_0^{\infty} m_1 \int_0^{a-2d_r} u\left(t - \frac{y-d_r}{v_f}\right) \\ &\times (1-m_1) dy\, dx + \int_0^{b_1} m_1 \int_{b_2}^{a-2d_r} u\left(t - \frac{a-y-d_r+x}{v_b}\right) m_2\, dy\, dx, \quad \text{where} \quad m_1 = \frac{\lambda_f+\lambda_b}{a-2d_r} e^{-(\lambda_f+\lambda_b)x}, \\ m_2 = &\ e^{-\lambda_c P_c (a-y-d_r+x)}, b_1 = \frac{a v_b - d_r(v_f+3v_b)}{v_f},\ b_2 = \frac{(a-d_r-y+x)v_f + d_r v_b}{v_b+v_f}. \end{aligned} \tag{17}$$

$$Term_1 = \begin{cases} k_5 + k_{34}\lambda(k_{10}+k_{13}) & if\ \ a \le k_1\ \ and\ \ k_{15} \le k_2 \\ k_6 + k_{34}\lambda(k_9+k_{13}) & if\ \ a > k_1\ \ and\ \ k_{15} \le k_2 \\ k_5 + k_{34}\lambda\,(k_{18}+k_{10}+k_8) & if\ \ a \le k_1\ \ and\ \ k_{11} \le k_4 \\ k_6 + k_{34}\lambda\,(k_{18}+k_9+k_8) & if\ \ a > k_1\ \ and\ \ k_{11} \le k_4 \\ k_5 + k_{34}\lambda\,(k_7+k_{17}+k_{10}+k_{12}-k_{16}) & if\ \ a \le k_1\ \ and\ \ k_{11} \ge k_4\ \ and\ \ k_3 < k_{14} \\ k_6 + k_{34}\lambda\,(k_7+k_{17}+k_{12}+k_9-k_{16}) & if\ \ a > k_1\ \ and\ \ k_{11} \ge k_4\ \ and\ \ k_3 < k_{14} \end{cases} \tag{18}$$

Moreover, the term $Pr(I = 0|X = x, Y = y)$, the probability that the carrier vehicle will not leave the highway over the distance $(y - d_r)$ is proposed in [5] as follows

$$Pr(I = 0|X = x, Y = y) = 1 - e^{-\lambda_c P_c(a-y-d_r+x)}. \quad (15)$$

Therefore, the second term on the right side of Eq. (4) can be obtained as follows,

$$Pr(T \le t, I = 0) = \int_0^{\infty} f(x, y) \int_0^{a-2d_r} u\left(t - \frac{y - d_r}{v_f}\right) \times (1 - e^{-\lambda_c P_c(a-y-d_r+x)}) dy \; dx \quad (16)$$

Using Eq. (4), Eq. (12), and Eq. (16), we can obtain an expression for the CDF of the vehicle-to-drone packet delivery delay as given in Eq. (17), as shown at the bottom of the previous page.

Finally, we obtained a closed-form expression for the first three terms in Eq. (17) (they include $u(t - \frac{y-d_r}{v_f})$ factors in the integrands) which is shown in Eq. (18), as shown at the bottom of the previous page. Moreover, the closed-form expression for the last term in Eq. (17) (which has a $u\left(t - \frac{a-y-d_r+x}{v_b}\right)$ factor) is given in Eq. (19), as shown at the bottom of this page.

where

$$k_1 = 3d_r + v_f t,\; k_2 = \frac{t^2\,(128\,d_r - 64a + 64tv_b)^2}{256},\; k_3 = (32768\,d_r - 1638a + 16384tv_b)^2,$$

$$k_4 = 4t\left(v_b k_{29} + t(v_b + v_f)\left(v_f + \frac{d_r - a/2 + tv_b/2 + k_{29}/(2v_b + 2v_f)}{t}\right)^2\right),$$

$$k_5 = (\lambda_f + \lambda_b)k_{33}\left(\frac{a - 2d_r}{\lambda_f + \lambda_b} + k_{19} - \frac{k_{27}e^{a\lambda_c P_c - 2d_r\lambda_c P_c}}{\lambda_c P_c k_{30}}\right), k_6 = \lambda k_{33}\left(k_{19} + \frac{d_r + tv_f}{\lambda} - \frac{k_{22}k_{27}}{\lambda_c P_c k_{30}}\right),$$

$$k_7 = \frac{k_{20} - k_{20}k_{25}e^{\lambda_c P_c k_{28}}}{k_{21}\lambda_c P_c},\; k_8 = \frac{k_{20}k_{26}\left(k_{23} - e^{-\lambda_c P_c k_{29}/(v_f+v_b)}\right)}{k_{21}\lambda_c P_c},\; k_9 = \frac{k_{26}(k_{22} - 1)}{k_{30}\lambda_c P_c}, k_{10} = \frac{k_{26}\left(e^{\lambda_c P_c(a-2d_r)} - 1\right)}{k_{30}\lambda_c P_c},$$

$$k_{11} = \frac{\left(2d_r(v_f + v_b) - k_{32} - a(v_f + v_b) + v_f(a - d_r) + d_r v_b + tv_b(v_f + v_b)\right)^2}{v_f + v_b},\; k_{12} = \frac{k_{22}(k_{25} - k_{26})}{\lambda_c P_c k_{30}},$$

$$k_{13} = \frac{k_{26}(k_{22} - 1)(k_{23} - 1)}{\lambda_c P_c k_{30}},\; k_{14} = 1073741824\,k_{24},\; k_{15} = 64k_{24},\; k_{16} = \frac{(k_{25} - k_{26})}{\lambda_c P_c k_{30}},\; k_{17} = \frac{(k_{25} - 1)}{\lambda_c P_c k_{30}},$$

$$k_{18} = \frac{(k_{26} - 1)}{\lambda_c P_c k_{30}},\; k_{19} = \frac{k_{27}}{\lambda_c P_c k_{30}},\; k_{20} = e^{\frac{k_{31}\lambda_c P_c}{v_f + v_b}},\; k_{21} = \lambda + \lambda_c p_c - \frac{\lambda p_c v_f}{v_f + v_b},\; k_{22} = e^{\lambda_c P_c(d_r + v_f t)},\; k_{23} = e^{-\left(\frac{k_{29}k_{30}}{v_f}\right)},$$

$$k_{24} = \left(d_r - a/2 + v_b t/2 + v_f t\right)^2,\; k_{25} = e^{-k_{28}k_{30}(v_f+v_b)/v_f},\; k_{26} = e^{k_{29}k_{30}/v_f},\; k_{27} = e^{-\lambda_c P_c(a-dr)},\; k_{28} = d_r + v_f t - \frac{k_{31}}{v_f + v_b},$$

$$k_{29} = v_f(a - d_r) - k_{32} + d_r v_b,\; k_{30} = \lambda + \lambda p_c,\; k_{31} = v_f(a - d_r) + d_r v_b,\; k_{32} = (v_f + v_b)(a - 2d_r),$$

$$k_{33} = \frac{1}{a - 2d_r}, k_{34} = k_{33}k_{27},\; \lambda = \lambda_f + \lambda_b.$$

$$Term_2 = \begin{cases} -k_6 k_{30}\lambda\left(k_{15} + \frac{k_{19}k_{21}(k_{18} - e^{-k_{24}\lambda_c P_c/(v_f+v_b)})}{k_{20}}\right) & \text{if } k_{11} \le k_{10} \\ -k_6 k_{30}\lambda u(v_b t - dr)\left(\frac{k_{23}(k_{14}-1)}{\lambda_c P_c k_{26}} + \frac{k_8 k_9 e^{a\lambda_c P_c} - e^{(d_r k_{26} - k_{26}v_b t + a\lambda_c P_c - 2d_r\lambda_c P_c)}}{k_7}\right) & \text{if } k_4 \le k_{28} + d_r v_f \text{ and } k_1 \le k_2 \text{ and } k_{10} \le k_{11} \\ -k_6 k_{30}\lambda\left(k_{15} + \frac{k_8 k_{21} - e^{a\lambda_c P_c}(k_{17} - k_{18})}{k_7}\right) & \text{if } k_4 \ge k_{28} + d_r v_f \text{ and } k_1 \le k_2 \text{ and } k_{10} \le k_{11} \\ -k_6 k_{30}\lambda\left(k_{16} - k_{12} + \frac{k_{19}}{k_{20}} + \left(\frac{k_{23}(k_{22} - k_{14})}{\lambda_c P_c k_{26}} - \frac{k_8 k_9 e^{a\lambda_c P_c}(k_{13} - e^{(-k_{14}\lambda_c P_c(d_r - tv_b))})}{k_7}\right)\left(0.5 sign\left(2d_r - a + \frac{k_{26} + d_r v_f + v_b v_f t}{v_f + v_b}\right) - 0.5\right)\right) & \text{if } k_3 \le k_5 \text{ and } k_4 \le k_{28} + d_r v_f \text{ and } k_1 \le k_2 \text{ and } k_{10} \le k_{11} \\ -k_6 k_{30}\lambda\left(k_{16} - k_{12}\frac{k_{23}(k_{21} - k_{12})}{\lambda_c P_c k_{26}} + \frac{k_{19}}{k_{20}} + \frac{k_8 k_9 e^{a\lambda_c P_c}(k_{13} - k_{17}k_{21})}{k_7}\right) & \text{if } k_3 \le k_5 \text{ and } k_4 \ge k_{28} + d_r v_f \text{ and } k_1 \le k_2 \text{ and } k_{10} \le k_{11} \end{cases} \quad (19)$$

TABLE 2. Simulation parameters.

Simulation Parameter	Value
a (km)	6
Exit Probability P_c	0.03
Road junctions density λ_c	0.002
v_f (m/s)	25
v_b (m/s)	30
Simulation runs	500
Simulation time (seconds)	600
Vehicles' communication range (m)	250
Channel date rate (Mbps)	2
Drone altitude (m)	300
Drone communication range (m)	550

V. DRONES-ACTIVE SERVICE

There are many papers that have proposed routing protocols for VANET communications based on a location service as in [22]–[24]. The main role of the location service is to obtain the updated locations of vehicles. Many papers have proposed designs of this location service such as HLS [15], and GLS [16].

In this paper, a drones-active service (DAS) is proposed. The DAS is a computational service that is based on the location service. By using the proposed closed-form expression, the service operator provides the number of drones needed to serve the VANET over the highway in the lowest vehicular density e.g., at the night period. However, DAS switches on some of these drones according to the vehicular density λ_f, λ_b changes and vehicle exit probability at the road junctions P_c.

In a realistic VANET scenario, the vehicular density and the vehicle exit probability at the road junctions change with the time. For instance, at the junction of a big company or a city, the probability of vehicle exit in the morning (people go to their work) or the end of the day (people return back from their work) is higher than other times (during the night).

The proposed DAS detects the vehicular density of the highway after every specified time period. In addition, DAS has the values of the probability of vehicle exit at different times. Then, based on the vehicle-to-drone delivery delay constraint, the detected vehicular density, and the the probability of vehicle exit at that time, DAS uses our proposed closed-form expression to obtain the maximum distance between two adjacent drones satisfying the delay constraint.

After that, the DAS finds the required number of drones for the highway at that time based on the calculated maximum distance. Finally, if the maximum distance increases, the DAS switches off some drones e.g., requiring their batteries to be recharged, and the other drones change their location based on the calculated maximum distance between them. On the contrary, if the maximum distance decreases, the DAS switches on some drones again to reach the required number of drones for the highway at that time.

However, in the obtained closed-form expression, the maximum distance is not on the right side. Therefore, after detection of the new value for the vehicular density, DAS can increase/decrease the current distance with d meters, and check the CDF threshold. If the CDF is more

where

$$k_1 = 64\,t^2\left(d_r - 0.5a + v_b t + 0.5\,tv_f\right)^2,\ k_2 = \frac{t^2\left(128\,d_r - 64a + 64v_f t\right)^2}{256},$$

$$k_3 = \frac{v_f\left(d_r(v_f+v_b) - a(v_f+v_b) + v_f(a-d_r) + d_r v_b + tv_b(v_f+v_b)\right)}{(v_f+v_b)},\ k_4 = v_f(a-d_r) + d_r v_b + tv_f v_b,$$

$$k_5 = -\frac{v_b\left(2d_r(v_f+v_b) - a(v_f+v_b) + v_f(a-d_r) + d_r v_b\right)}{(v_f+v_b)},\ k_6 = e^{-\lambda_c P_c(a-dr)},\ k_7 = \lambda_c\lambda_c P_c,\ k_8 = e^{-\lambda_c P_c v_b t},$$

$$k_9 = e^{-d_r\lambda_c P_c},\ k_{10} = 4t(v_b+v_b)\left(v_f(a-d_r) - k_{28} + d_r v_b + t\left(v_b + \frac{2d_r - a + tv_f + \frac{k_{24}}{v_f} - \frac{k_{24}}{v_f+v_b}}{2t}\right)^2\right),$$

$$k_{11} = (v_f + v_b(2d_r - a + t_v f + \frac{k_{24}}{v_f} + \frac{k_{24}}{v_f+v_b})^2 + 4\,k_{24}v_f t,\ k_{12} = \frac{k_{22}k_{19}e^{-\left(\frac{k_{25}\lambda_c P_c v_f}{k_{27}(v_f+v_b)}\right)}}{k_{20}},\ k_{13} = k_2 e^{-k_{25}\lambda_c P_c/k_{27}},$$

$$k_{14} = e^{k_{26}(d_r - v_b t)},\ k_{15} = \frac{k_{23}(k_{21}-1}{\lambda_c P_c k_{26}},\ k_{16} = \frac{k_{23}(k_{22}-1}{\lambda_c P_c k_{26}},\ k_{17} = e^{-k_{24}\lambda_c P_c/v_f},\ k_{18} = e^{-k_{24}k_{26}/v_f},$$

$$k_{19} = e^{k_{29}\lambda_c P_c/(v_f+v_b)},\ k_{20} = \lambda P_c\left(\lambda + \lambda_c P_c - \frac{\lambda P_c v_f}{v_f+v_b}\right),\ k_{21} = e^{k_{24}k_{26}/v_f},\ k_{22} = e^{k_{26}k_{25}/k_{27}},\ k_{23} = e^{\lambda_c P_c(a-d_r)},$$

$$k_{24} = v_f(a-d_r) - k_{28} + d_r v_b,\ k_{25} = d_r - a + tv_b + \frac{k_{29}}{v_f+v_b},\ k_{27} = \frac{v_f}{v_f+v_b},\ k_{28} = (a-2d_r)(v_f+v_b),$$

$$k_{29} = v_f(a-d_r) + d_r v_b,\ \lambda = \lambda_f + \lambda_b.$$

Algorithm 1 DAS

Input: vehicular densities λ_f, λ_b, delay constraint $T_{\max}$, distance value that increased/decreased every iteration *step*, drone communication range d_r, exit probability P_c, expected number of junctions λ_c, a table has the maximum distance and the related parameters that are calculated before by DAS *distancetable*, and violation probability ϵ.

procedure START
  while (*true*) **do**
    detect λ_f, λ_b from the location service
    $T_m \leftarrow T_{\max}$, $stepdis \leftarrow step$
    $d_r \leftarrow drone.range\,(Pathloss_{th}, altitude)$
    $drones_{on} \leftarrow$ count $(current\ active\ drones)$
    $drones_{off} \leftarrow$count $(current\ inactive\ drones)$
    $threshold \leftarrow \epsilon$
    $distancetable \leftarrow table(P_c, \lambda_f, \lambda_b)$
    if $(P_c, \lambda_f, \lambda_b) \in distancetable$ **then**
      $distance = distancetable[P_c, \lambda_f, \lambda_b]$
      go to calcdrones
    end if
    $T_c \leftarrow$ Proposed.form $(\lambda_f, \lambda_b, P_c, d_r, distance)$
    while $(|T_c - T_m| > threshold)$ **do**
      if $T_c < T_m$ **then**
        $distance = distance - stepdis$
      else
        $distance = distance + stepdis$
      end if
      $T_c \leftarrow$ Proposed.form $(\lambda_f, \lambda_b, P_c, d_r, distance)$
    end while
    $distancetable.add(\lambda_f, \lambda_b, P_c, d_r, distance)$
calcdrones:
    $drones_{req} = highwaylength/distance$
    if $drones_{req} > drones_{on}$ **then**
      switchon (difference ($drones_{req}$, $drones_{on}$))
    else
      switchoff (difference ($drones_{req}$, $drones_{on}$))
    end if
  end while
end procedure

than/less than the threshold, DAS can increase/decrease the distance another time by d meters. Then, the algorithm repeats this step until it reaches the CDF delay threshold. The distance in that iteration is the maximum distance between two adjacent drones satisfying the delay constraint. Then, DAS saves this maximum distance and the related parameters (vehicular distance, vehicle exit probability) in a table to use them directly.

Next, DAS decides which drones will be off/on based on this distance. The first priority is for the drone that needs to recharge or closest to consuming its battery. Secondly, if all drones have equal battery charges or they depend on solar energy and do not need to recharge, all drones move the same distance. Then, the drones at the end of the highway will be turned off. When λ decreases again, each drone returns to the last position and these drones are switched on again.

This method benefits from the mobile nature of the drones and VANET. The DAS approach takes into account the temporal vehicular density variation and the probability of vehicle exit. DAS helps to ensure the minimum number of active drones that can satisfy the required constraint on the vehicle-to-drone packet delivery delay. DAS can switch off some drones that need to recharge their batteries or based on any other configuration. Algorithm 1 explains the DAS in detail.

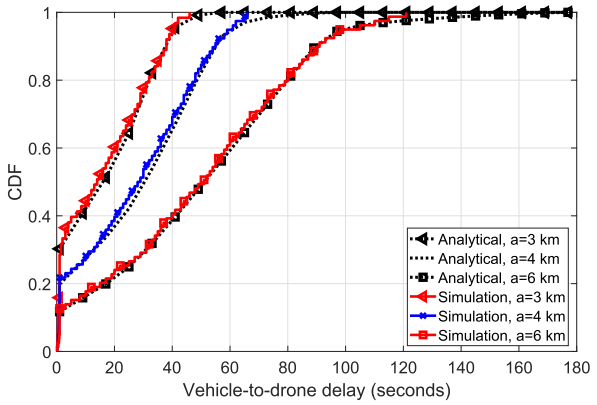

FIGURE 5. Vehicle-to-drone delay with changing *a*.

VI. SIMULATION AND MODEL VALIDATION

This section compares our simulation results against those from our analysis. We implement our proposed protocol in NS-2 (v. 2.34). In addition, we use VanetMobiSim [25] to generate realistic vehicle mobilities with considering the mobility model mentioned in Section III. In this mobility model, a bi-directional highway segment is considered. Table 2 summarizes the configuration parameters used in the simulation. The following subsections presents the results for simulations and the analysis with different parameters (the vehicular density, drone density, junctions density, probability of exit at junction, and the forward and backward speeds). However, for clarity of the plots, we include the plots for the simulations in Fig. 5 only. It was found through simulation that the accuracy in the others figures were similar to those in Fig. 5.

A. DRONE DENSITY

Fig. 5 shows the analytical and simulation results for the CDF of the vehicle-to-drone packet delivery delay with the same simulation parameters as in Table 2, while changing the distance between each two drones a to values of (a = 3, 4, and 6) km. In Fig. 5, the analytical results are plotted using the closed-form in Eq. (17).

It can be seen that the two curves (analytical, simulation) agree closely across all time values for all figures, indicating that our analysis is accurate in characterizing the CDF of the the vehicle-to-drone packet delivery delay. However, a small deviation between the analytical and simulations results may be observed. This is because our anal-

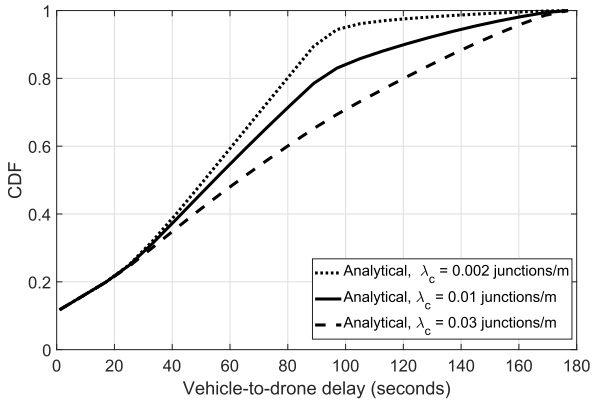

FIGURE 6. Vehicle-to-drone delay with changing junction density λ_c.

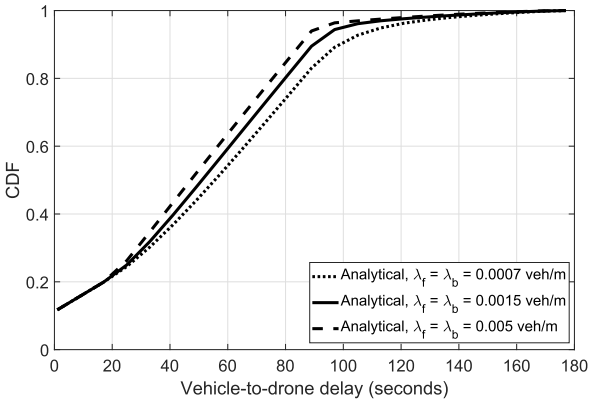

FIGURE 7. Vehicle-to-drone delay with changing vehicular density.

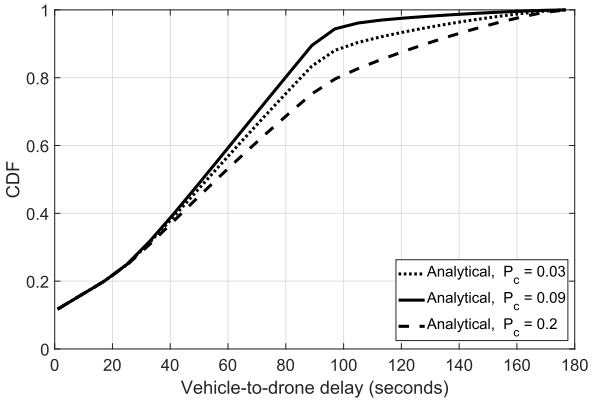

FIGURE 8. Vehicle-to-drone delay with changing P_c.

ysis focuses on the worst case where the original packet is stored by its source vehicle, or the next vehicle in the opposite direction, until it is within communication range of a drone. However, the source vehicle may forward the packets to a neighboring vehicle. As a result, the vehicle-to-drone packet delivery delay decreases. In addition, our analysis assumes that the time required for a vehicle to receive and process a message before it is available for further relaying is negligible. The small deviations increase in the case of a high vehicular density because in that case, the probability of forwarding the packet to a neighbor vehicle is increased. However, this case is beyond the scope of this paper.

In addition, one can note that a (drone density) highly impacts the CDF of the vehicle-to-drone packet delivery delay. With increasing the drone density, the CDF of the vehicle-to-drone packet delivery delay increases for all values of the drone density. For instance, the CDF of the vehicle-to-drone packet delivery delay at a equal to 3 km is the highest CDF for the all values of t. This is because increasing the drones density leads to a decrease in a. As a result, the source vehicle carries the packet for a shorter distance. Consequently, the vehicle-to-drone packet delivery delay decreases.

B. JUNCTION DENSITY

Fig. 6 shows the analytical results for the CDF of the vehicle-to-drone packet delivery delay with the same parameters as in Table 2, while changing the junction density λ_c to values of (0.002, 0.01, and 0.03) junctions/m.

The results show that the junction density λ_c impacts the CDF of the vehicle-to-drone packet delivery delay. By increasing the junction density, the CDF of the vehicle-to-drone packet delivery delay decreases for all values of the drone density. For instance, the CDF of the vehicle-to-drone packet delivery delay for λ_c equal to 0.03 junctions/m is the lowest CDF for the all values of t. This is because increasing the junction density leads to an increase in the probability that the vehicle (packet carrier) exits from the highway at any of those junctions. As a result, the drone receives the second replica from the packet that takes a longer time to reach the next drone. Consequently, the vehicle-to-drone packet delivery delay increases.

C. VEHICULAR DENSITY

Fig. 7 shows the analytical results for the CDF of the vehicle-to-drone packet delivery delay with the same parameters as in Table 2, while changing the vehicular density λ_f and λ_b to values of (0.0007, 0.0015, and 0.005) vehicles/m.

In addition, one can note that the vehicular densities λ_f and λ_b impact the CDF of vehicle-to-drone packet delivery delay. By increasing the vehicular density, the CDF of the vehicle-to-drone packet delivery delay increases for all values of time. For instance, the CDF of the vehicle-to-drone packet delivery delay at 0.005 veh/m is the highest CDF for the all values of t. This is because increasing the vehicular density decreases the vehicle-to-drone distance and the time required to forward the packet to a drone.

D. EXIT PROBABILITY

Fig. 8 shows the analytical results for the CDF of the vehicle-to-drone packet delivery delay with the same parameters as in Table 2, while changing the probability of exit P_c to values of (0.03, 0.09, and 0.2).

One can note that the probability of exit P_c impacts the CDF of vehicle-to-drone packet delivery delay. By increasing

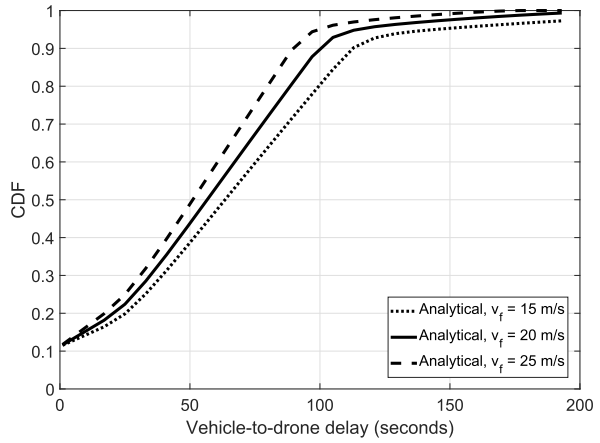

FIGURE 9. Vehicle-to-drone delay with changing v_f.

the vehicular density, the CDF of the vehicle-to-drone packet delivery delay decreases for all values of P_c. For instance, the CDF of the vehicle-to-drone packet delivery delay at P_c equal to 0.2 is the lowest CDF for the all values of t. This is because increasing the probability of exit leads to an increase in the probability that the vehicle (packet carrier) exits from the highway at any junctions. As a result, the drone receives the second replica from the packet that takes a longer time to reach the next drone. Consequently, the vehicle-to-drone packet delivery delay increases.

E. FORWARD SPEED

Fig. 9 shows the analytical results for the CDF of the vehicle-to-drone packet delivery delay with the same parameters as in Table 2, while changing the forward speed v_f to values of (15, 25, and 35) m/s.

Results show that the forward speed has an impact on the CDF of vehicle-to-drone delivery delay. With increasing v_f, the CDF of the vehicle-to-drone packet delivery delay increases for all values of v_b. For instance, the CDF of the vehicle-to-drone delivery delay at $v_f = 35$ m/s is the highest CDF for all values of t considered. This is expected because increasing v_f causes an decrease in the time required to reach the drone in the forward direction.

F. BACKWARD SPEED

Fig. 10 shows the analytical results for the CDF of the vehicle-to-drone packet delivery delay with the same parameters as in Table 2, while changing the backward speed v_b to values of (10, 20, and 30) m/s.

Results show that the backward speed has an impact on the CDF of vehicle-to-drone delivery delay. With increasing v_b, the CDF of the vehicle-to-drone packet delivery delay increases for all values of v_b. For instance, the CDF of the vehicle-to-drone delivery delay at v_b equal to 30 m/s is the highest CDF for all values of t. This is expected because increasing v_b causes an decrease in the time required to reach the drone in the backward direction. As a result, the vehicle-to-drone delivery delay decreases.

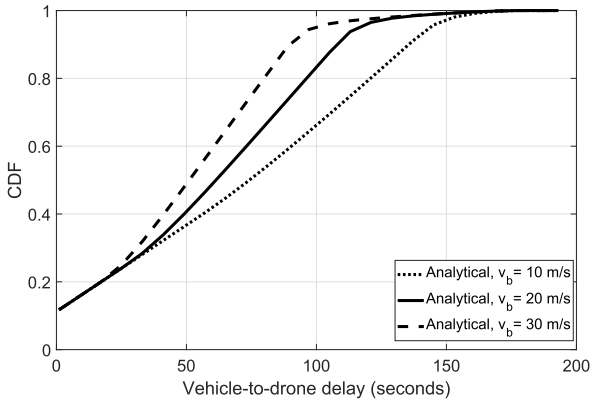

FIGURE 10. Vehicle-to-drone delay with changing v_b.

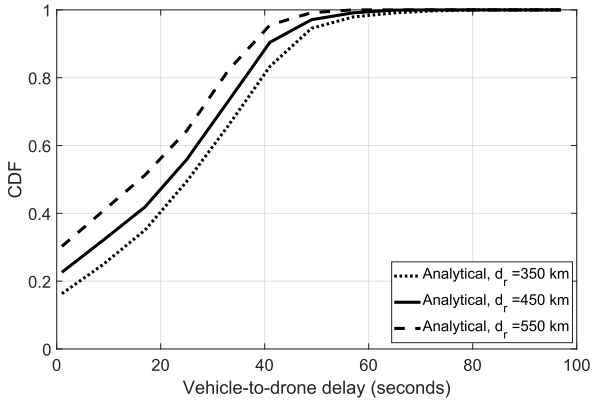

FIGURE 11. Vehicle-to-drone delay with changing d_r.

G. DRONE COMMUNICATION RANGE

Fig. 11 shows the analytical results for the CDF of the vehicle-to-drone packet delivery delay with the same parameters as in Table 2, and $x = 3$ km,while changing the drone communication range d_r to values of (350, 450, and 550) m.

Results show that the value of the drone communication range d_r has an impact on the CDF of the vehicle-to-drone delivery delay. With increasing the d_r, the CDF of the vehicle-to-drone packet delivery delay increased for all values of d_r. For instance, the CDF of the vehicle-to-drone delivery delay at d_r equal to 550 m is the highest CDF for the all values of t. This is because an increase in d_r while keeping the distance between a vehicle and a drone constant, results in a lower distance necessary for the message to forward the packets to the drone.

H. RESULTS COMPARED WITH THE PREVIOUS WORK

Our model is a generalization of the model in [5]. Our model considers the drone communication range d_r in the model. On the contrary, [5] considers a zero communication range for the RSUs. Therefore, our model's results are equal to those in [5] in the case that both models use a constant velocity model except when d_r equals zero.

On the other hand, to make sure the expression is not linear, we compare our results to those in [5], but subsitiute the

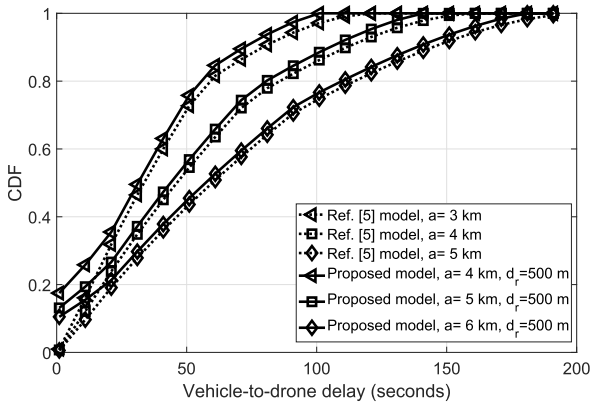

FIGURE 12. Results compared with the previous work.

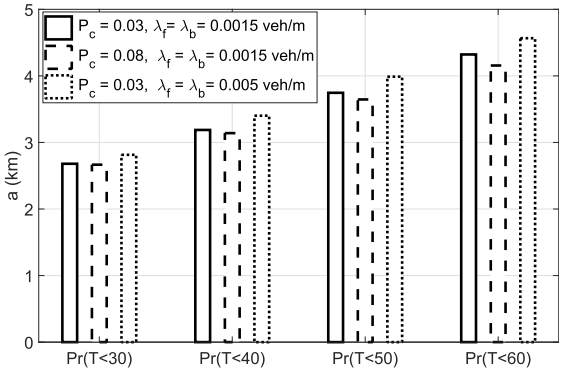

FIGURE 13. DAS simulation results.

value of a in [5] by $(a - 2d_r)$. Fig. 12 compares the results from the proposed analysis and that from [5] for the CDF of the vehicle-to-drone packet delivery delay with the same parameters as in Table 2, while changing the drone range a to values of (4, 5, and 6) km.

The results show there is a big difference at t=0. In our model, we consider the drone range. Therefore, when the source vehicle is located within the drone range, the vehicle-to-drone range is zero as we assume the delay for wireless communication is zero. Therefore, in our model, the CDF of vehicle-to-drone delay at t equal zero is greater than zero for all values of a. However, [5] considers a zero wireless communication range for the RSUs. Therefore, the CDF of the vehicle-to-drone delay at t=0 is close to zero for all values of a.

I. DAS SIMULATION RESULTS

We implemented the DAS algorithm in NS-2 based on the proposed closed-form expression and the maximum of the objective function mentioned in Eq. 3 $(1 - F_T(T_{\max}, a) \leq \epsilon)$. Fig. 13 shows the simulation results of the DAS algorithm at different vehicular densities and probability of exit with the same parameters as in Table 2, and ϵ equal 0.006 while changing $T_{\max}$ to values of (30, 40, 50, and 60) seconds. Analytical results are not added here, as we use the analytical closed form inside the simulation, giving the same result.

Results show that the value of $T_{\max}$ has a high impact on a. With increasing $T_{\max}$, the value of a increases for all values of $T_{\max}$. For instance, the highest values of a are at $T_{\max}$ equal to 60 seconds. This is because an increase in $T_{\max}$ leads to a longer a that still satisfies the probability delay constraint. As a result, the number of required drones will be different based on the new values of a, where the drone density equals $1/a$.

VII. CONCLUSION

In this paper, we proposed a routing protocol that uses infrastructure drones for boosting VANET communications to achieve a minimum vehicle-to-drone packet delivery delay. This paper proposed a closed-form expression for the probability distribution of the vehicle-to-drone packet delivery delay on a two-way highway. In addition, based on that closed-form expression, we calculated the minimum drone density (maximum separation distance between two adjacent drones) that stochastically limits the worst case of the vehicle-to-drone packet delivery delay. Moreover, we proposed a drones-active service (DAS) that is added to the location service in a VANET to dynamically and periodically obtain the required number of active drones based on the current highway connectivity state by obtaining the maximum distance between each two adjacent drones while satisfying a probabilistic constraint for vehicle-to-drone packet delivery delay. The simulation results show the accuracy of our analysis and reflect the relation between the drone density, vehicular density and speed, other VANET parameters, and the vehicle-to-drone packet delivery delay. In our future work, we will consider infrastructure-less drones with V2V communication. In addition, we will formulate the problem as an optimization problem to achieve the minimum end-to-end delay for V2V communication with a minimum number of drones. Moreover, we will formulate an optimization problem to obtain the optimal placement for the drones in VANETs using DAS.

REFERENCES

[1] C. Kaplan, "GPS, cellular, FM speed and safety control devise," U.S. Patent 11 645 551, Dec. 26, 2006.
[2] C. Campolo and A. Molinaro, "Multichannel communications in vehicular ad hoc networks: A survey," *IEEE Commun. Mag*, vol. 51, no. 5, pp. 158–169, May 2013.
[3] B. Hassanabadi and S. Valaee, "Reliable periodic safety message broadcasting in VANETs using network coding," *IEEE Trans. Wireless Commun.*, vol. 13, no. 3, pp. 1284–1297, Mar. 2014.
[4] A. Abdrabou and W. Zhuang, "Probabilistic delay control and road side unit placement for vehicular ad hoc networks with disrupted connectivity," *IEEE J. Sel. Areas Commun.*, vol. 29, no. 1, pp. 129–139, Jan. 2011.
[5] A. Abdrabou, B. Liang, and W. Zhuang, "Delay analysis for sparse vehicular sensor networks with reliability considerations," *IEEE Trans. Wireless Commun.*, vol. 12, no. 9, pp. 4402–4413, Sep. 2013.
[6] J. Jeong, S. Guo, Y. Gu, T. He, and D. H. C. Du, "Trajectory-based data forwarding for light-traffic vehicular ad hoc networks," *IEEE Trans. Parallel Distrib. Syst.*, vol. 22, no. 5, pp. 743–757, May 2011.
[7] J. He, L. Cai, J. Pan, and P. Cheng, "Delay analysis and routing for two-dimensional vanets using carry-and-forward mechanism," *IEEE Trans. Mobile Comput.*, vol. 16, no. 7, pp. 1830–1841, Jul. 2017.

[8] C.-C. Lin and D.-J. Deng, "Optimal two-lane placement for hybrid VANET-sensor networks," *IEEE Trans. Ind. Electron.*, vol. 62, no. 12, pp. 7883–7891, Dec. 2015.
[9] C. Liu, H. Huang, and H. Du, "Optimal RSUs deployment with delay bound along highways in VANET," *J. Combinat. Optim.*, vol. 33, no. 4, pp. 1168–1182, 2017.
[10] I. Bor-Yaliniz and H. Yanikomeroglu, "The new frontier in RAN heterogeneity: Multi-tier drone-cells," *IEEE Commun. Mag.*, vol. 54, no. 11, pp. 48–55, Nov. 2016.
[11] X. Wang, L. Fu, Y. Zhang, X. Gan, and X. Wang, "VDNet: An infrastructure-less UAV-assisted sparse VANET system with vehicle location prediction," *Wireless Commun. Mobile Comput.*, vol. 16, no. 17, pp. 2991–3003, 2016.
[12] O. S. Oubbati, A. Lakas, N. Lagraa, and M. B. Yagoubi, "CRUV: Connectivity-based traffic density aware routing using UAVs for VANets," in *Proc. IEEE ICCVE*, Oct. 2015, pp. 68–73.
[13] O. S. Oubbati, A. Lakas, N. Lagraa, and M. B. Yagoubi, "UVAR: An intersection UAV-assisted VANET routing protocol," in *Proc. IEEE WCNC*, Apr. 2016, pp. 1–6.
[14] R. Shahidi and M. H. Ahmed, "Probability distribution of end-to-end delay in a highway VANET," *IEEE Commun. Lett.*, vol. 18, no. 3, pp. 443–446, Mar. 2014.
[15] W. Kieß, H. Füßler, J. Widmer, and M. Mauve, "Hierarchical location service for mobile ad-hoc networks," *ACM SIGMOBILE Mobile Comput. Commun. Rev.*, vol. 8, no. 4, pp. 47–58, 2004.
[16] J. Li, J. Jannotti, D. S. J. De Couto, D. R. Karger, and R. Morris, "A scalable location service for geographic ad hoc routing," in *Proc. ACM MobiCom*, 2000, pp. 120–130.
[17] A. Al-Hourani, S. Kandeepan, and A. Jamalipour, "Modeling air-to-ground path loss for low altitude platforms in urban environments," in *Proc. IEEE GLOBECOM*, Dec. 2014, pp. 2898–2904.
[18] I. Bor-Yaliniz, S. S. Szyszkowicz, and H. Yanikomeroglu, "Environment-aware drone-base-station placements in modern metropolitans," *IEEE Wireless Commun. Lett.*, to be published, doi: 10.1109/LWC.2017.2778242.
[19] M. Mozaffari, W. Saad, M. Bennis, and M. Debbah, "Drone small cells in the clouds: Design, deployment and performance analysis," in *Proc. IEEE GLOBECOM*, Dec. 2015, pp. 1–6.
[20] A. Al-Hourani, S. Kandeepan, and S. Lardner, "Optimal LAP altitude for maximum coverage," *IEEE Wireless Commun. Lett.*, vol. 3, no. 6, pp. 569–572, Dec. 2014.
[21] H. Fernández, L. Rubio, V. M. Rodrigo-Peñarrocha, and J. Reig, "Path loss characterization for vehicular communications at 700 MHz and 5.9 GHz under LOS and NLOS conditions," *IEEE Antennas Wireless Propag. Lett*, vol. 13, pp. 931–934, 2014.
[22] P. Sermpezis, G. Koltsidas, and F. N. Pavlidou, "Investigating a junction-based multipath source routing algorithm for VANETs," *IEEE Commun. Lett.*, vol. 17, no. 3, pp. 600–603, Mar. 2013.
[23] M. Ayaida, H. Fouchal, L. Afilal, and Y. Ghamri-Doudane, "A comparison of reactive, grid and hierarchical location-based services for vanets," in *Proc. IEEE VTC*, Sep. 2012, pp. 1–5.
[24] M. Jerbi, S. M. Senouci, T. Rasheed, and Y. Ghamri-Doudane, "Towards efficient geographic routing in urban vehicular networks," *IEEE Trans. Veh. Technol.*, vol. 58, no. 9, pp. 5048–5059, Nov. 2009.
[25] J. Härri, F. Filali, C. Bonnet, and M. Fiore, "VanetMobiSim: Generating realistic mobility patterns for VANETs," in *Proc. ACM VANET*, 2006, pp. 96–97.

HAFEZ SELIEM received the B.Sc. and M.Sc. degrees from Ain Shams University, Cairo, Egypt, in 2009 and 2014, respectively. He is currently pursuing the Ph.D. degree with Faculty of Engineering and Applied Science, Memorial University of Newfoundland, St John's, NL, Canada. His research interests include wireless multihop networks, vehicular *ad hoc* networks, mobile *ad hoc* networks, and software design.

REZA SHAHIDI received the M.Eng. and Ph.D. degrees in computer engineering with a specialization in image processing from the Memorial University of Newfoundland in 2003 and 2008, respectively. He was a Post-Doctoral Fellow with The University of British Columbia from 2008 to 2009, where he conducted research on seismic imaging. He spent several years with an industry in radar signal and image processing. Since 2015, he has been a Research Associate with the Memorial University of Newfoundland. His research interests include vehicular networks, digital signal and image processing, and ocean remote sensing.

MOHAMED HOSSAM AHMED received the Ph.D. degree in electrical engineering from Carleton University, Ottawa, ON, Canada, in 2001. From 2001 to 2003, he was a Senior Research Associate with Carleton University. In 2003, he joined the Faculty of Engineering and Applied Science, Memorial University of Newfoundland, where he is currently a Full Professor. He is a Registered Professional Engineer in the province of Newfoundland, Canada. He has authored over 140 papers in international journals and conferences. His research interests include radio resource management in wireless networks, multi-hop relaying, cooperative communication, vehicular *ad hoc* networks, cognitive radio networks, and wireless sensor networks. His research was supported by NSERC, CFI, QNRF, Bell/Aliant, and other governmental and industrial agencies. He received the Ontario Graduate Scholarship for Science and Technology in 1997, the Ontario Graduate Scholarship in 1998, 1999, and 2000, and the Communication and Information Technology Ontario Graduate Award in 2000. He served as the Co-Chair for the Signal Processing Track in 2014 ISSPIT, the Transmission Technologies Track in VTC2010-Fall, and the Multimedia and Signal Processing Symposium in 2009 CCECE. He serves as an Editor for the IEEE Communications Surveys and Tutorials. He serves as an Associate Editor for the *International Journal of Communication Systems* (Wiley) and the *Wireless Communications and Mobile Computing* (Wiley). He served as a Guest Editor for a special issue on Fairness of Radio Resource Allocation, the EURASIP JWCN in 2009, a special issue on Radio Resource Management in Wireless Internet, and the *Wireless Communications and Mobile Computing* (Wiley) Journal in 2003.

MOHAMED S. SHEHATA received the B.Sc. degree (Hons.) and the M.Sc. degree in computer engineering from Zagazig University, Egypt, in 1996 and 2001, respectively, and the Ph.D. degree in software engineering from the University of Calgary, Canada, in 2005. He was as a Post-Doctoral Fellow with the University of Calgary on a joint project between the University of Calgary and the Canadian Government, called Video Automatic Incident Detection. He joined Intelliview Technologies, Inc., as a Vice-President of the Research and Development Department. In 2013, after seven years with the industry, he joined the Faculty of Engineering and Applied Science, MUN, as an Assistant Professor of computer engineering. His research interests include courses in computer vision, image processing, data structures, programming, and software design.